Journal of King Saud University – Computer and Information Sciences 31 (2019) 113–124

Contents lists available at ScienceDirect

Journal of King Saud University – Computer and Information Sciences

journal homepage: www.sciencedirect.com

A new exponentially directional weighted function based CT image denoising using total variation

Manoj Kumar, Manoj Diwakar *

Babasaheb Bhimrao Ambedkar University, Lucknow, India

ARTICLE INFO

Article history:
Received 31 August 2016
Revised 7 December 2016
Accepted 8 December 2016
Available online 22 December 2016

Keyword:
Total variation
Computed tomography
Image denoising
Anisotropic function
Isotropic function

ABSTRACT

Today, Computed tomography (CT) is one of the high efficient tools in medical science which helps to diagnose the human body. The presence of noise may degrade the visual quality of the CT images, especially for low contrast images. Therefore, we propose a method based on the modification of total variation (TV) for noise suppression in CT images which is helpful to preserve the clinically relevant details. The modification of TV is performed by introducing a new exponentially directional weighted function (EDWF), which is based on the difference between L_1 and L_2 norms over the exponential function. Furthermore, a numerical algorithm is designed to solve the minimization problem of EDWF using Split Bregman method. The experimental results of proposed scheme are visually analyzed over the real noise CT image, added noise in true CT images, and also on low contrast zoomed noisy CT image. Apart from visual analysis, the proposed scheme is also verified with some standard performance metrics (RMSE, PSNR, SSIM, ED, DIV and GMSD). The proposed scheme is also compared with some standard existing methods and it is observed that performance of proposed scheme is superior to existing methods in terms of visual quality and performance metrics.

1. Introduction

Computed tomography is one of the important tools which helps to depict the problem of human body (Trinh et al., 2012; Muller et al., 2012; Bhadauria and Dewal, 2012; Zhu et al., 2012) such as fractures, brain hemorrhage, lung cancer and many more. The CT images help to find the medical relevant details for diagnosis purpose. Therefore, a clean medical image is required to get the correct medical relevant contents. However, various studies confirm that CT images are generally degraded by noise which can affect the medical relevant details, especially on the low contrast images. Due to the presence of noise, a medical image may not give an accurate analysis which may be harmful for the patients. Various reasons have been found for occurrence of noise in CT images such as low photon absorption, data loss during acquisition and transmission, software and hardware limitation, mathematical computations and low radiation dose. It can be analyzed from the literature (Gravel et al., 2004; Sanches et al., 2008; Attivissimo et al., 2010; Andria et al., 2013; Sun et al., 2013) that the type of noise in CT images is generally an additive white Gaussian noise. The image denoising is one of the solutions to suppress the noise from noisy images, but the main challenge of image denoising is to preserve the details of the images such as edges, contrasts, texture, corners and small structures. The main goal of image denoising in CT images is to improve the medical images visually by reducing the noise and preserving details as much as possible.

Various techniques have been developed to remove the Gaussian noise in CT images such as window based thresholding using multi wavelet transform (Ali et al., 2010), self-similarity feature tissue based CT image denoising using Non-Local Means method (Wu et al., 2011, 2013a,b), Wavelet packet based image denoising (Fathi and Naghsh, 2012), a locally adaptive shrinkage rule in tetrolet domain for CT image denoising (Kumar and Diwakar, 2016), wavelet based noise reduction in CT-Images using similarity analysis (Borsdorf et al., 2008), Wiener filtering based medical image denoising using dual tree complex thresholding wavelet transform

* Corresponding author.
E-mail addresses: mkjnuiitr@gmail.com (M. Kumar), manoj.diwakar@gmail.com (M. Diwakar).
Peer review under responsibility of King Saud University.

Production and hosting by Elsevier

https://doi.org/10.1016/j.jksuci.2016.12.002
1319-1578/

(Naimi et al., 2015) and many more. Some other new algorithms (Hu et al., 2013a,b, 2016) are also introduced for image denoising where image denoising is performed based on the concept of Mean Square Error. These algorithms give noise suppressed image and help to recover the missing structures of the noisy images.

Recently, various methods have been studied to remove the Gaussian noise by least square fidelity minimization (Hu et al., 2011a,b, 2012; Yan and Wu-Sheng, 2015). In least square fidelity minimization, the authors (Hu et al., 2011a) enhanced the $L_p - L_2$ formulation with the concept of soft shrinkage for image denoising. Further, this work is extended using $L_p - L_2$ formulation with a power-iterative strategy to provide the smoothness using the discontinuity of the global minimizer concept (Hu et al., 2011b). Similarly, a weighted TV (WTV) method (Yan and Wu-Sheng, 2015) is also used to denoise the images by estimating the weight value over the TV regularization function. To minimize the least square fidelity term, many regularization functions have been investigated such as Tikohonov, anisotropic diffusion and Total variation methods. Tikohonov method (Tikhonov and Arsenn, 1977; Andrews and Hunt, 1997) is the simplest one in which data fidelity term is minimized with L_2 norm regularization, but it over smooths the detail parts of images (Dobson and Santosa, 1996; Nikolova, 2000). To overcome that, anisotropic diffusion method has been proposed to enhance the details of the images by stopping the diffusion at the edges, but it blurs the noisy edges (Catt et al., 1992; Esedoglu and Osher, 2004). In parallel with anisotropic diffusion (Perona and Malik, 1990; Weickert, 1998), Total variation (TV) based regularization was proposed to overcome the smoothness from the noisy images. From various studies, it can be found that TV method performs better for noise suppression in medical images, but it has a problem of unwanted stair-artifacts (Dobson et al., 1995; Vogel and Oman, 1996; Catt et al., 1994; Chambolle and Pock, 2011). The advantages of TV and anisotropic diffusion were combined to improve the drawbacks of TV method and the combination is called anisotropic total variation method (Rudin et al., 1992).

Rudin-Osher-Fatemi (R.O.F.) model (Rudin et al., 1992) was proposed to provide the smooth and denoise image by TV method using L_2 norm fidelity optimization. The authors (Rudin et al., 1992) also discussed the computational difficulty because of nonlinearity and non-differentiability. Therefore, R.O.F. model is further modified to avoid these difficulties and improved the performance of image denoising (Chambolle, 2004). A non-differential TV method was introduced using Bregman iteration and got the success to minimize the problems. Later, Bregman iteration was improved using linearization function (Goldstein and Osher, 2009). Further, it was extended to minimize the L_1 regularization by introducing Split Bregman method (Li et al., 2012; Osher et al., 2005; Yin et al., 2008; Denis et al., 2009). Recently, various methods (Cai et al., 2009a,b,c; Chen et al., 2015; Candes et al., 2008 have been proposed using Split Bregman method by modifying norms as well as regularization terms. Some authors also proposed the mixed models such as $L_2 - L_1$ (Zibulevsky and Elad, 2012; Lou et al., 2015), higher degree based image denoising (Hu and Jacob, 2012) and gradient-based algorithms for constrained total variation (Beck and Teboulle, 2009). However, the results of mixed model based image denoising are improved over the classical TV method and some of the state-of-the-art methods, but still blocking effects are observed near the noisy edges. To solve the blocking effects in TV model, a method (Sun et al., 2015) was proposed based on exponential TV method. Further, image denoising is performed by Split Bregman using exponential TV function. This method gives better noise reduction.

In Jiang et al. (2015) and Bayram and Kamasak (2012)), the authors addressed the directional derivatives of an image and image denoising is performed on the basis of choosing directional TV function. The directional derivatives give better edge and texture preservation. Recently, total variation methods were improved such as coefficients driven total variation (Al-Ameen and Sulong, 2014), nonnegativity constrained TV (Landi et al., 2012) and so on, to attenuate the noise from the noisy CT images.

The main concept of image denoising is to suppress the noise and preserve the edges from the noisy images. Unfortunately, the previous methods (Hu et al., 2011a; Goldstein and Osher, 2009; Sun et al., 2015; Bayram and Kamasak, 2012; Al-Ameen and Sulong, 2014; Landi et al., 2012) have not preserved well structures while suppression of noise over the noisy images. Therefore, to suppress the noise with better edge preservation, we propose a method for CT image denoising using total variation method, where an exponentially directional weight function is introduced using $L_2 - L_1$, directional derivatives and exponential function. Two advantages of $L_2 - L_1$ over other nonconvex measures are its Lipschitz regularity, and guarantee of convergence, which is analogous to a convex splitting technique for gradient systems. The directional derivatives and exponential function help to provide better edge preservation and more smoothness over the noisy pixels, respectively. The main contribution of this article is to develop an exponentially directional weighted function using the difference between anisotropic and isotropic functions for CT image denoising. Further, Split Bregman method is used to solve the minimization problem of the exponentially directional weighted function.

The organization of this article is as follows: Section 2 describes a brief introduction on total variation. In Section 3, the proposed exponentially directional weighted total variation model and its numerical algorithm based on Split Bregman algorithm is described in detail. The Experimental results and comparisons are discussed in Section 4. Finally, the conclusions are drawn in Section 5.

2. Background of total variation

Total variation is one of the popular models to develop the optimization algorithms for solving sparse representation problem which was originally developed for image denoising by Rudin, Osher, and Fatemi (R.O.F.) (Rudin et al., 1992). A general model for such problem is:

$$R = \min_U TV(U) + \frac{\mu}{2}\|U - F\|^2 \tag{1}$$

where, $TV(U)$ is the regularization term as a total variation (TV), μ is a positive parameter to control $TV(U)$, $\|U - F\|^2$ is the fidelity term, and $||.||$ represents L_2 norm. R is the optimal solution or the reconstructed result. This is a simple and convex optimization model. To solve the optimization problem, firstly, the Gradient projection method (Rudin et al., 1992) is used to accelerate the convergence using fixed point or variable splitting algorithms. Further, more efficient techniques were also developed such as Newton's method (Dobson et al., 1995), dual formulation based TV denoising method (Chambolle and Pock, 2011Goldstein and Osher, 2009). Generally, TV model follows a pair of directions: horizontal and vertical directions. Many authors (Jiang et al., 2015; Bayram and Kamasak, 2012) gave the privilege to the edges along the directions for image denoising. Some authors (Bayram and Kamasak, 2012) used the trigonometric functions to reweight the horizontal and vertical directions to smooth the noisy regions of the images. In fidelity term, L_2 norm is the most common norm which was used to reduce the Gaussian noise and it works well in image denoising (Nikolova, 2000; Landi et al., 2012; Yan and Wu-Sheng, 2015). However, if some of the pixels are degraded by the non-Gaussian type noise,

then those pixels are not properly denoised with these methods. Few authors (Darbon and Sigelle, 2006) have also used fidelity term with L_1 norm for the non-Gaussian type of noisy images.

TV model is widely used in image processing for various applications such as image deblurring (Chen et al., 2015), denoising (Al-Ameen and Sulong, 2014), etc. The formulation of TV model can categorized as: isotropic and anisotropic TV, which are used as a regularization term for sparse representation problems. The total variation (TV) can be defined as the sum of L_1 or L_2 norm of the gradients for all the pixels.

An anisotropic TV model is denoted by $TV^{(A)}$, and can be expressed as:

$$TV^{(A)}(U) = \sum_{ij}(|\nabla_x U(i,j)|) + (|\nabla_y U(i,j)|) \tag{2}$$

where, $|.|$ represents L_1 norm.

An isotropic TV model is denoted by $TV^{(I)}$, and can be expressed as:

$$TV^{(I)}(U) = \sum_{ij}\sqrt{(\nabla_x U(i,j))^2 + (\nabla_y U(i,j))^2} \tag{3}$$

where, $\nabla_x U$ and $\nabla_y U$ are the horizontal and vertical gradients, respectively.

3. Proposed methodology

Generally, the distribution of noise in CT images follows the Poisson distribution due to statistical fluctuations on X-ray projected data (Muller et al., 2012). However, different reconstruction algorithms can change the distribution of noise models. Thus by Central Limit Theorem (CLT), the noise can be best modeled by the Gaussian distribution. The CLT can be applied in CT images because of addition of values from many different projections into the voxels of CT images (Kumar and Diwakar, 2016).

Here, with the assumption that the CT images are corrupted by the Gaussian noise with zero mean and different variances, the scheme is proposed using total variation model. However, TV method has been proven to be quite efficient for suppression of the Gaussian noise in images. But it has a tendency to remove certain image details and texture along with the noise. The requirement for the proposed scheme is that the regularization function should be an increasing function with respect to the smoothness of the image. At the same time, considering numerical algorithm of the minimization, it is highly expected that the regularization functional should be in simple form as possible. Therefore, an exponentially directional weighted function (EDWF) is proposed using anisotropic and isotropic total variations, which is discussed below in the first subsection. Further, a numerical algorithm is designed to solve the minimization problem of EDWF using Split Bregman method (Goldstein and Osher, 2009) for CT image denoising, discussed in second subsection.

The noisy CT image (F) can be expressed as:

$$F = U + \eta \tag{4}$$

where, U is the clean image to be estimated from F and η is an additive white Gaussian noise.

3.1. Exponentially directional weighted function (EDWF)

The basic idea of re-weighting of the total variation function is to enhance the sparsity which was originally introduced in Candes et al. (2008). Here, a new exponentially directional weighted function (EDWF) for anisotropic and isotropic TV is introduced.

The directional derivatives ($\nabla_S U$) are computed as:

$$\nabla_S U(i,j) = \begin{cases} \nabla_a U(i,j) = U(i,j) - U(i-1,j) \\ \nabla_b U(i,j) = U(i,j) - U(i+1,j) \\ \nabla_c U(i,j) = U(i,j) - U(i-2,j) \\ \nabla_d U(i,j) = U(i,j) - U(i+2,j) \\ \nabla_e U(i,j) = U(i,j) - U(i,j-1) \\ \nabla_f U(i,j) = U(i,j) - U(i,j+1) \\ \nabla_g U(i,j) = U(i,j) - U(i,j-2) \\ \nabla_h U(i,j) = U(i,j) - U(i,j+2) \end{cases} \tag{5}$$

where $S \in \{a,b,c,d,e,f,g,h\}$. The mean of the absolute derivatives is calculated as:

$$E(i,j) = \frac{\sum_{i,j}|\nabla_S U(i,j)|}{K} \tag{6}$$

where K is the total number of directional derivatives. These directional derivatives are responsible to preserve the structures in the images such as edges. Using these directional derivatives over the noisy pixels, an exponentially directional weighted function (EDWF) is introduced to suppress the noise from CT images.

The exponentially directional weighted functions (EDWF) are defined, as:

$$\alpha = e^{(-|(|E(i,j)|-\gamma||E(i+1,j)||))|)} \tag{7}$$

$$\beta = e^{(-|(|E(i,j)|-\gamma||E(i,j+1)||))|)} \tag{8}$$

where, γ is a diagonal dominant weight factor which is used as a control parameter. It can be estimated by obtaining the similarity between horizontal and vertical directions, and can be expressed as Borsdorf et al. (2008):

$$\gamma = \frac{2.E(i+1,j).E(i,j+1)}{E^2(i+1,j) + E^2(i,j+1)} \tag{9}$$

The values of weights (α and β) and diagonal dominant weight factor (γ) are normalized between 0 and 1. According to similarity factor, the weight values (α and β) are attenuated differently. When average value of γ is close to 0, weight values (α and β) behave like $e^{-(|L_1|)}$. If it is close to 1, weight values (α and β) behave like $e^{-(|L_1-L_2|)}$.

In the proposed method, the original oscillation measure ∇U is modified using exponential weighted function. The motivation of using exponential functional is that, the exponential energy curve emphasizes more on the noisy pixels, because as the value of $L_2 - L_1$ increases, the exponential curve increases faster than the $L_2 - L_1$. As higher energy is penalized, the smoothness of noisy pixels is increased. In addition, when the value of $L_2 - L_1$ is zero, the slope value of the energy curve may become zero or near to zero due to more pixels with the same intensity value. This means as the energy decreases, the difference between pixels becomes smaller, which leads to the blocking effect, whereas, the exponential function with $L_2 - L_1 = 0$ assures that the pixels can still exchange intensities even when their intensity values are very close to each other which reduces blocking effect up-to a certain degree.

Let, the total variation (TV) be defined with EDWF in horizontal and vertical gradients, $\nabla_x U$ and $\nabla_y U$, respectively. The anisotropic TV denoted by $TV^{(A)}_{EDWF}$ can be expressed as:

$$TV^{(A)}_{EDWF}(U^l) = \sum_{ij}\alpha(i,j)(|\nabla_x U^l(i,j)|) + \beta(i,j)(|\nabla_y U^l(i,j)|) \tag{10}$$

and, isotropic TV denoted by $TV^{(I)}_{EDWF}$ can be expressed as:

$$TV^{(I)}_{EDWF}(U^l) = \sum_{ij}\sqrt{\alpha(i,j)(\nabla_x U^l(i,j))^2 + \beta(i,j)(\nabla_y U^l(i,j))^2} \tag{11}$$

where, $\alpha(i,j) > 0$ and $\beta(i,j) > 0$ are the weights which effectively allow to convert the nonconvex total variation into the convex total variation. The major role of exponentially directional weighted function (EDWF) is to keep TV_{EDWF} to convex as long as possible. l is the number of iterations to estimate the re-weighted values for the TV_{EDWF} minimization. Following is the proposed iterative reweighted algorithm to solve the TV minimization problem.

Algorithm 1. Iterative reweighted TV minimization

1. Initialize the parameters: μ, l, and set $\alpha(i,j) = \beta(i,j) = 1$.
2. Compute directional derivatives $\nabla_S U$.
3. For l number of iteration, solve the TV_{EDWF} regularized problem as, $\min_U TV_{EDWF}(U) + \frac{\mu}{2}\|U - F\|^2$ and update values of $\nabla_S U, \alpha(i,j)$ and $\beta(i,j)$.
4. Repeat step 3 for next iteration.
5. Terminate; When l iterations are completed.

In Algorithm 1, Step 3 has to solve the minimization problem. To solve the minimization problem for both anisotropic and isotropic TV, Split Bregman iteration method is used, as discussed in the following subsection.

3.2. Split Bregman Iteration to solve EDWF problem

The Split Bregman method has several good properties such as it can converge very quickly when applied to the L_1 regularization problem and avoid the problem of numerical instabilities (Goldstein and Osher, 2009).

3.2.1. Anisotropic TV denoising

We begin with anisotropic total variation to solve the minimization problem of Algorithm 1 for CT image denoising, as follows:

$$\min_U \left|\nabla_x^{EDWF} U\right| + \left|\nabla_y^{EDWF} U\right| + \frac{\mu}{2}\|U - F\|^2 \tag{12}$$

where, $\nabla_x^{EDWF} U = \alpha(i,j)(U(i,j) - U(i+1,j))$ and $\nabla_y^{EDWF} U = \beta(i,j)(U(i,j) - U(i,j+1))$.

Here in the Eq. (12), first and second terms are the total variation regularizers, third is the fidelity norm and $\mu > 0$ is the weighted function to control the regularizer and fidelity terms.

Let, Bregman Splitting method be applied to solve the above minimization problem. First, $\nabla_x^{EDWF} U$ and $\nabla_y^{EDWF} U$ are replaced by d_x and d_y, respectively. This yields the constrained problem as:

$$\min_U |d_x| + |d_y| + \frac{\mu}{2}\|U - F\|^2, s.t.\ d_x = \nabla_x^{EDWF} U,\ d_y = \nabla_y^{EDWF} U \tag{13}$$

By enforcing the constraints, the above equation turns into unconstrained optimization problem, as,

$$\min_{d_x,d_y,U} |d_x| + |d_y| + \frac{\mu}{2}\|U - F\|^2 + \frac{\lambda}{2}\|d_x - \nabla_x^{EDWF} U - b_x^l\|^2 + \frac{\lambda}{2}\|d_y - \nabla_y^{EDWF} U - b_y^l\|^2 \tag{14}$$

where, b_x^l and b_y^l are updated through the Bregman iteration, as follows:

$$b_x^{(l+1)} = b_x^l + \nabla_x^{EDWF} U^{(l+1)} - d_x^{(l+1)} \tag{15}$$

$$b_y^{(l+1)} = b_y^l + \nabla_y^{EDWF} U^{(l+1)} - d_y^{(l+1)} \tag{16}$$

To obtain $U^{(l+1)}, d_x^{(l+1)}$ and $d_y^{(l+1)}$, the above equations can be written as follows:

$$u^{(l+1)} = \arg\min_U \frac{\mu}{2}\|U - F\|^2 + \frac{\lambda}{2}\|d_x^l - \nabla_x^{EDWF} U - b_x^l\|^2 + \frac{\lambda}{2}\|d_y^l - \nabla_y^{EDWF} U - b_y^l\|^2 \tag{17}$$

$$d_x^{(l+1)} = \arg\min_{d_x} |d_x| + \frac{\lambda}{2}\|d_x^l - \nabla_x^{EDWF} U^{(l+1)} - b_x^l\|^2 \tag{18}$$

$$d_y^{(l+1)} = \arg\min_{d_y} |d_y| + \frac{\lambda}{2}\|d_y^l - \nabla_y^{EDWF} U^{(l+1)} - b_y^l\|^2 \tag{19}$$

To solve Eq. (17) a method as suggested in Yan and Wu-Sheng (2015) is used to get the first order optimal condition for weighted TV regularization. Therefore, the first order optimal condition for weighted TV regularization can be written as:

$$\left\{\mu + \lambda\left(\nabla_x^{EDWF}\right)^T \nabla_x^{EDWF} + \lambda\left(\nabla_y^{EDWF}\right)^T \nabla_y^{EDWF}\right\} U^{l+1} = \mu F + \lambda \nabla_x^{EDWF}(d_x^l - b_x^l) + \lambda \nabla_y^{EDWF}\left(d_y^l - b_y^l\right) \tag{20}$$

where, $(\nabla_x^{EDWF})^T$ and $(\nabla_y^{EDWF})^T$ are the adjoint matrices of ∇_x^{EDWF} and ∇_y^{EDWF}.

Eq. (20) can be solved using the Gauss–Seidel method because the system is strictly diagonal dominant, therefore,

$$U^{l+1}(i,j) = \frac{\psi}{\xi} \tag{21}$$

where, $\psi = \mu F + \lambda \nabla_x^{EDWF}(d_x^l - b_x^l) + \lambda \nabla_y^{EDWF}(d_y^l - b_y^l) + \lambda[\alpha^2(i,j)U^l(i+1,j)] + \alpha^2(i-1,j)U^{l+1}(i-1,j) + \beta^2(i,j)U^l(i,j+1) + \beta^2(i,j-1)U^{l+1}(i,j-1)$- and $\xi = \mu + \lambda[\alpha^2(i,j) + \alpha^2(i-1,j) + \beta^2(i,j) + \beta^2(i,j-1)]$

To solve the coupling problem in elements of d_x and d_y, both d_x and d_y are computed using shrinkage rule, as given below:

$$d_x^{l+1} = sgn(\tau_x).max(|\tau_x| - 1/\lambda, 0) \tag{22}$$

$$d_y^{l+1} = sgn(\tau_y).max(|\tau_y| - 1/\lambda, 0) \tag{23}$$

where, $\tau_x = \nabla_x^{EDWF} U^{(l+1)} + b_x^l$ and $\tau_y = \nabla_y^{EDWF} U^{(l+1)} + b_y^l$.

3.2.2. Isotropic TV denoising

Here, the convex problem is discussed to solve the exponentially directional weighted isotropic TV regularization using Split Bregman method, which can be expressed as:

$$\min_U \sum_{i,j} \sqrt{\{\nabla_x^{EDWF} U(i,j)\}^2 + \{\nabla_y^{EDWF} U(i,j)\}^2} + \frac{\mu}{2}||U - F||^2 \tag{24}$$

Similarly, as discussed in anisotropic TV denoising, the problem for exponentially directional weighted isotropic TV regularization using Split Bregman strategy can be formulated as:

$$\min_U \sum_{i,j} \sqrt{\{d_x(i,j)\}^2 + \{d_y(i,j)\}^2} + \frac{\mu}{2}\|U - F\|^2,\quad s.t.\ d_x = \nabla_x^{EDWF} U,\quad d_y = \nabla_y^{EDWF} U \tag{25}$$

By enforcing the constraints, the above equation turns into unconstrained optimization problem, as:

$$\min_{d_x,d_y,U} \sum_{i,j} \sqrt{\{d_x(i,j)\}^2 + \{d_y(i,j)\}^2} + \frac{\mu}{2}\|U - F\|^2 + \frac{\lambda}{2}\|d_x - \nabla_x^{EDWF} U - b_x^l\|^2 + \frac{\lambda}{2}\|d_y - \nabla_y^{EDWF} U - b_y^l\|^2 \tag{26}$$

To solve the above equation for l number of iterations, it can be rewritten as:

$$u^{(l+1)} = \arg\min_{U} \frac{\mu}{2}\|U-F\|^2 + \frac{\lambda}{2}\|d_x^l - \nabla_x^{EDWF}U - b_x^l\|^2 + \frac{\lambda}{2}\|d_y^l - \nabla_y^{EDWF}U - b_y^l\|^2 \quad (27)$$

$$\left(d_x^{(l+1)}, d_y^{(l+1)}\right) = \arg\min_{d_x,d_y} \sum_{i,j} \sqrt{\{d_x(i,j)\}^2 + \{d_y(i,j)\}^2} + \frac{\lambda}{2}\|d_x^l - \nabla_x^{EDWF}U^{(l+1)} - b_x^l\|^2 + \frac{\lambda}{2}\|d_y^l - \nabla_y^{EDWF}U^{(l+1)} - b_y^l\|^2 \quad (28)$$

As, in anisotropic case, the variables d_x and d_y are decoupled, but in anisotropic case, both variables are coupled. To solve this problem, a generalized shrinkage formula is used, as given below:

$$d_x^{(l+1)} = max(s^l - 1/\lambda, 0)\frac{\nabla_x^{EDWF}U^{(l)} + b_x^l}{s^l} \quad (29)$$

$$d_y^{(l+1)} = max(s^l - 1/\lambda, 0)\frac{\nabla_y^{EDWF}U^{(l)} + b_y^l}{s^l} \quad (30)$$

where, $s^l = \sqrt{|\nabla_x^{EDWF}U^{(l)} + b_x^l|^2 + |\nabla_y^{EDWF}U^{(l)} + b_y^l|^2}$

In the proposed method, exponentially directional weighted functions (α and β) are introduced for horizontal and vertical directions. These weighted functions are effectively used to modify the TV method for CT image denoising, as shown in Algorithm 1. Further, minimization problem of Algorithm 1 is solved using Split Bregman method.

4. Numerical Experiments

In this section, the numerical results are presented on some real CT images to verify the efficiency of proposed algorithm. Here in the experiments, two types of noisy CT images are used to analyze the performance of the proposed algorithm. The sample of real CT images shown in Fig. 1 is the first type of CT images, which are made noisy by adding an additive white Gaussian noise at various levels ($\sigma \in \{10, 20, 30, 40\}$). Fig. 2 represents noisy CT image data set with σ= 20. Another type of CT image is real noisy CT image as shown in Fig. 12(a) which is also used for experimental evaluation.

Both types of noisy CT images are of size 512 × 512 used to verify the performance of the proposed algorithm for the quantitative and qualitative evaluation. Images shown in Figs. 1(a-d) and 12(a) are collected from public access database (http://www.via.cornell.edu/visionx/). All experiments are evaluated in MATLAB 7.12 on Pentium Dual Core 2 GHz. For easy conversation, CT images in Figs. 1(a), (b), (c) and (d) are denoted as CT1, CT2, CT3 and CT4, respectively. From literature (Beck and Teboulle, 2009; Hu and Jacob, 2012) as well as from experimental evaluation, it is observed that in most of the cases anisotropic total variation gives better outcome or sometimes similar in comparison to isotropic TV. With this consideration, here all simulations are reported using anisotropic type of total variation. For all experiments, the maximum number of iterations l is set to 30, μ is .05 and λ is 2μ.

Since the comparative study is also required to show the ability of the proposed algorithm, some well-known standard methods are chosen for comparision, such as: directional total variation (DTV) (Bayram and Kamasak, 2012), coefficients-driven total variation (CDTV) (Al-Ameen and Sulong, 2014), nonnegativity constrained total variation (NCTV) (Landi et al., 2012), Split Bregman total variation (SBTV) (Goldstein and Osher, 2009), iterative reweighted TV_p algorithm (IRTV) (Hu et al., 2011a) and Exponential total variation (ETV) (Sun et al., 2015). For comparison analysis, the parameter values other than iteration number l, μ and λ are used as reported in corresponding literature, Bayram and Kamasak (2012), Al-Ameen and Sulong (2014), Landi et al. (2012), Goldstein and Osher (2009), Hu et al. (2011a) and Sun et al. (2015).

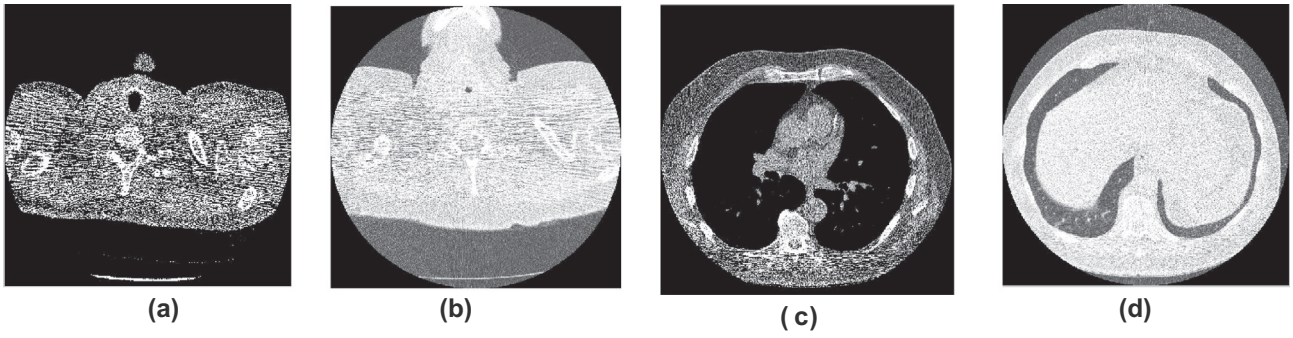

Fig. 1. Original CT image data set.

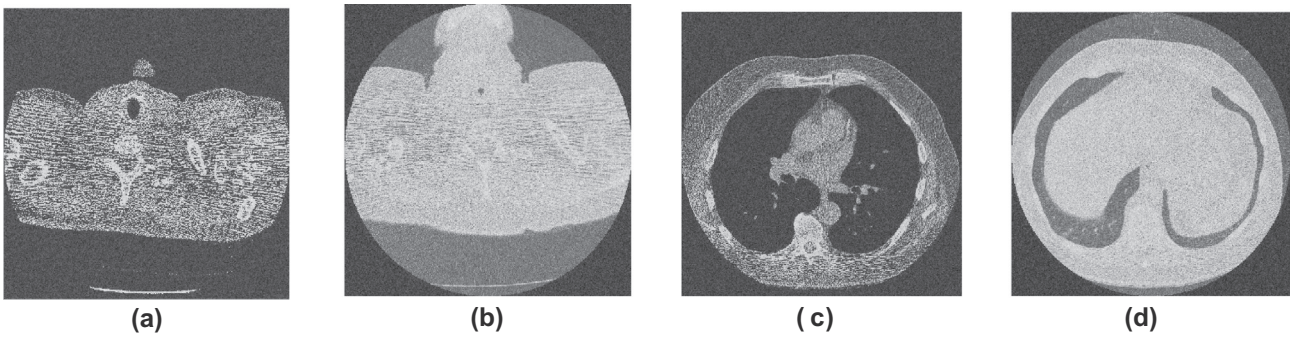

Fig. 2. Noisy CT image data set σ = 20.

To measure the accuracy of the proposed algorithm, some standard performance metrics are used, such as: root mean square error (RMSE), peak signal to noise ratio (PSNR), Structural Similarity (Zibulevsky et al., 2004) (SSIM), Entropy Difference (ED), Difference in Variance (DIV) and Gradient Magnitude Similarity Deviation (Xue et al., 2014 (GMSD). SSIM provides the accuracy on the basis of structural information, while GMSD gives the accuracy by estimating pixel-wise gradient similarity. The outcome of SSIM lies between −1 and 1, the value closer to 1 shows better results. However, GMSD values lie between 0 and 1, the value closer to 0 indicates better results.

Peak Signal-to-noise Ratio (PSNR) is an important factor to evaluate denoising performance. The high PSNR value represents more similarity between the denoising and original image than lower PSNR values. For clean image (X) and denoised image (R), the PSNR is expressed as:

$$PSNR = 10 \times log_{10}\left(\frac{255\times 255}{MSE}\right) \tag{31}$$

where, Mean Square Error (MSE) is defined as-

$MSE = \frac{1}{mn}\sum_{i=0}^{m-1}\sum_{j=0}^{n-1}[X(i,j) - R(i,j)]^2$

Root mean square error (RMSE) can be estimated as:

$$RMSE = \sqrt{MSE} \tag{32}$$

Entropy is a statistical measure of randomness that can be used to characterize the texture of the input images. Between clean image (X) and denoised image (R), patch wise Shannon entropy is estimated. The difference of mean value represents as Entropy Difference (ED). Entropy Difference (ED) is calculated as follows:

$$ED = SE(X) - SE(R) \tag{33}$$

where, SE represents Shannon entropy. Shannon entropy (SE) is calculated as follows, (Fathi and Naghsh, 2012):

$$SE = -\sum_i X_i^2 log(X_i^2) \tag{34}$$

The performance of algorithm can also be measured by estimating DIV, defined as follows:

$$DIV = 1 - \frac{Var(R)}{Var(X)} \tag{35}$$

where, $Var(R)$ is the variance of denoised image and $Var(X)$ is the variance of clean image. The values closer to 0 indicate better results of RMSE, ED and DIV.

Figs. 3–9 show the results of DTV, CDTV, NCTV, SBTV, IRTV, ETV and proposed algorithm, respectively. For real noisy CT image, Fig. 12(b), (c), (d), (e), (f), (g) and (h) show the results of DTV, CDTV, NCTV, SBTV, IRTV, ETV and proposed algorithm, respectively. To measure the visual comparison, there is no mathematical or specific method available. Therefore, the results need to be evaluated with naked eye to determine the best filtered images. For better visual inspection, we follow four criteria: (i) visibility of the artifacts; (ii) preservation of edge details; (iii) visibility of low contrast objects, and (iv) preservation of the texture.

The performance metrics (RMSE, PSNR, SSIM, ED, DIV and GMSD) are also computed using various noise levels and shown in Tables 1 and 2. The best values among all the methods are shown in bold. The results shown in Tables 1 and 2 demonstrate that in most of the cases, the proposed method is superior to all other compared methods.

The results of DTV, NCTV and ETV are good in terms of noise reduction from noisy CT images. However, DTV method gives

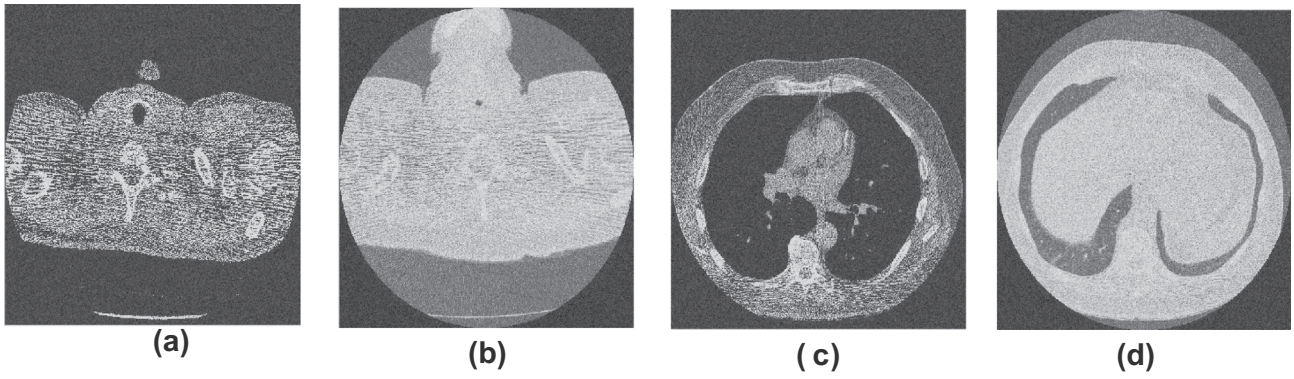

Fig. 3. Results of DTV.

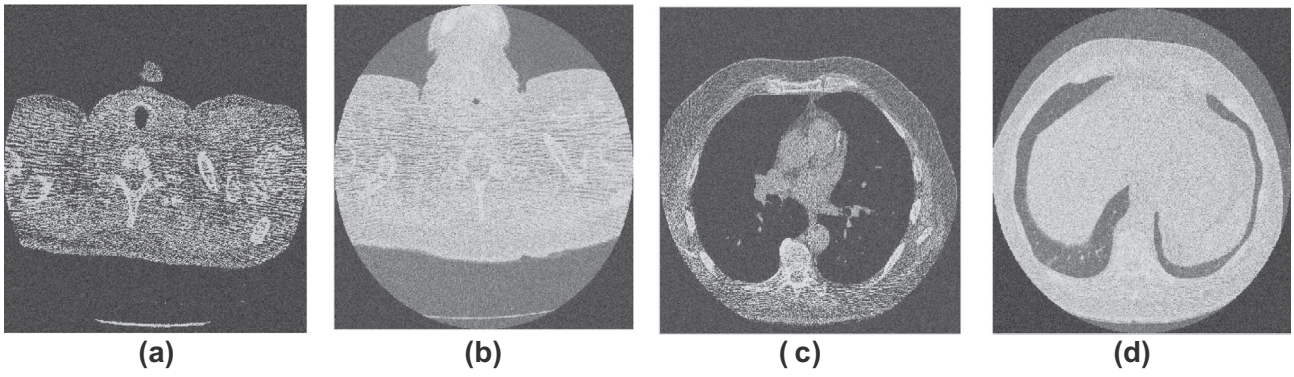

Fig. 4. Results of CDTV.

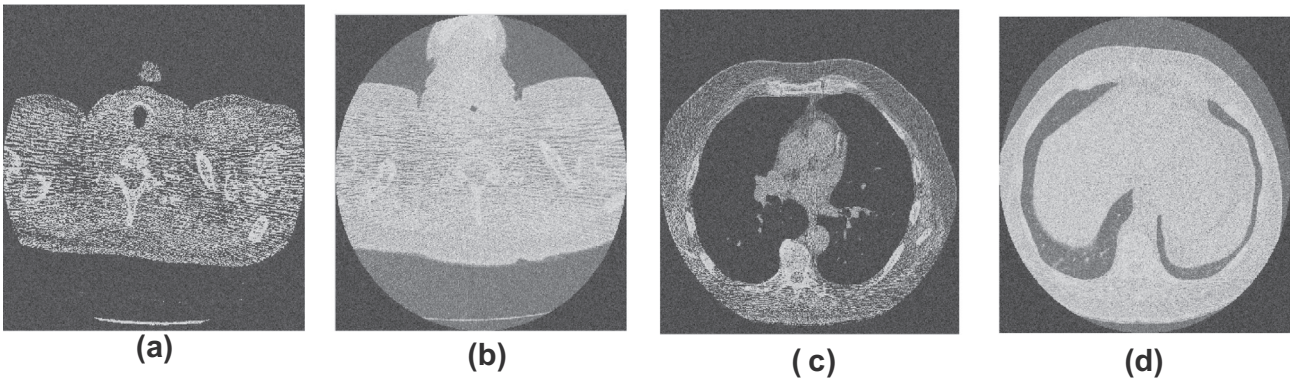

Fig. 5. Results of NCTV.

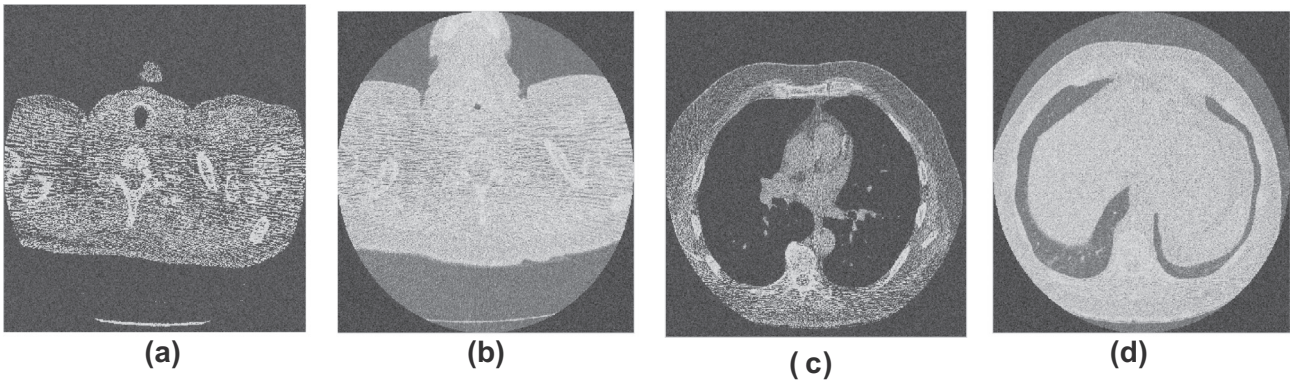

Fig. 6. Results of SBTV.

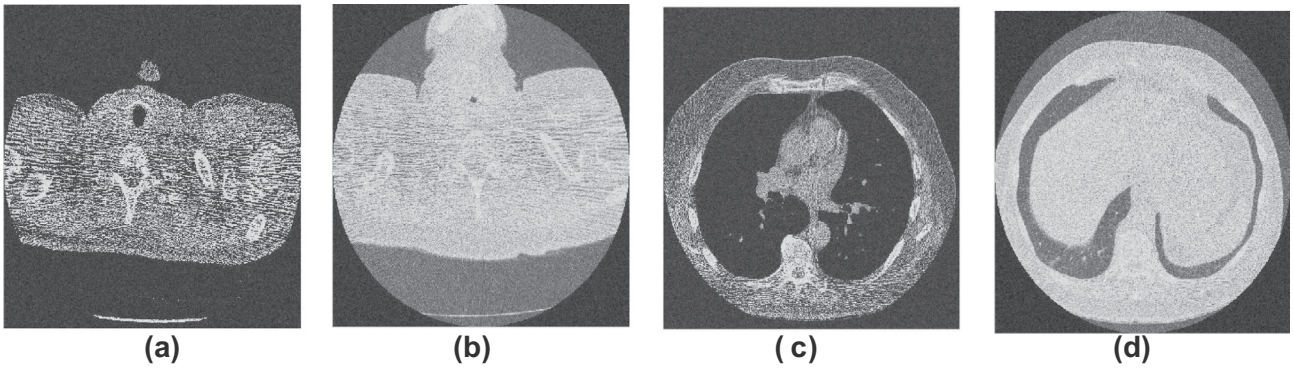

Fig. 7. Results of IRTV.

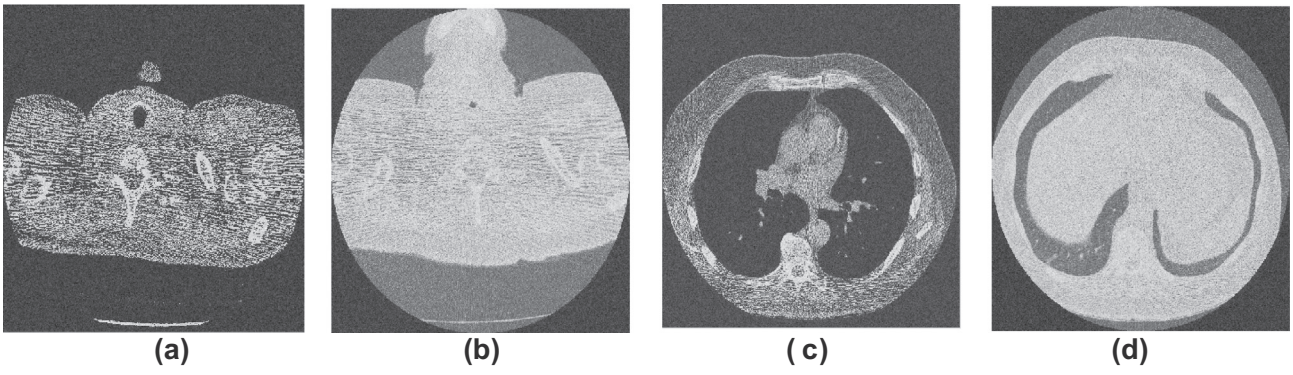

Fig. 8. Results of ETV.

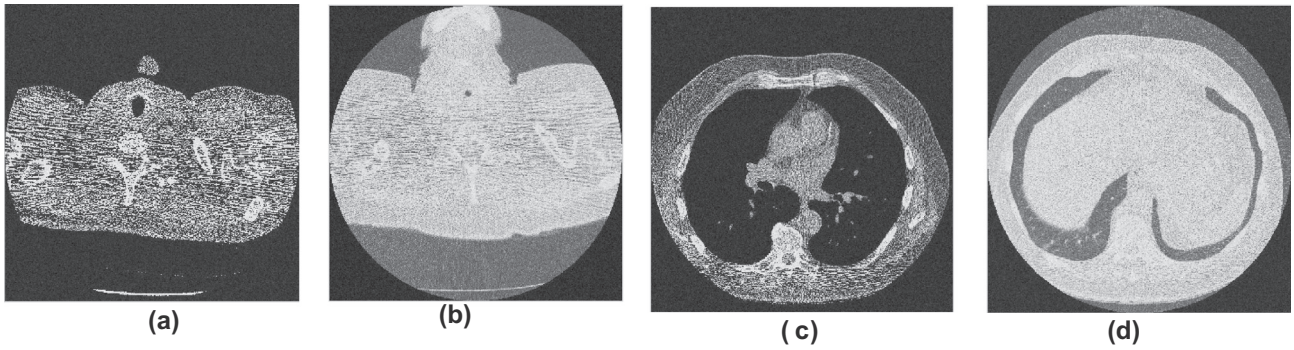

Fig. 9. Results of proposed scheme.

Table 1
RMSE, PSNR and SSIM of CT denoised images.

		RMSE				PSNR				SSIM			
Image	σ	10	20	30	40	10	20	30	40	10	20	30	40
CT1	DTV	8.1727	18.1708	28.0817	37.9911	29.8509	22.9115	19.1317	16.5074	0.8822	0.6992	0.6077	0.5592
	CDTV	8.5437	18.5204	28.4952	38.6414	29.4675	22.7472	19.0078	16.3576	0.8737	0.6963	0.6075	0.5576
	NCTV	9.2709	19.2453	29.1603	39.0873	28.7581	22.4145	18.7997	16.2564	0.8563	0.6871	0.6020	0.5550
	SBTV	9.9575	19.9490	29.9086	39.7625	28.1380	22.0987	18.5870	16.1113	0.8429	0.6776	0.5983	0.5519
	IRTV	7.4668	17.4150	27.4157	37.3013	30.6353	23.2813	19.3408	16.6642	0.8954	**0.7158**	0.6133	0.5634
	ETV	7.8725	17.8067	27.7561	37.7731	30.1796	23.0866	19.2330	16.5542	0.8879	0.7050	0.6109	0.5608
	Proposed	**6.9736**	**16.9260**	**26.8551**	**36.9188**	**31.2315**	**23.5284**	**19.5213**	**16.7543**	**0.9078**	0.7153	**0.6176**	**0.5637**
CT2	DTV	8.1692	18.1343	28.0820	38.0104	29.8539	22.9272	19.1310	16.5018	0.9385	0.8061	**0.6989**	0.5856
	CDTV	8.5778	18.4709	28.5423	38.4462	29.4308	22.7662	18.9880	16.4016	0.9344	0.8021	0.6816	0.5788
	NCTV	9.2620	19.2230	29.1711	39.0849	28.7628	22.4219	18.8004	16.2565	0.9250	0.7926	0.6741	0.5730
	SBTV	9.9451	19.9060	29.9458	39.8759	28.1481	22.1194	18.5722	16.0855	0.9157	0.7822	0.6659	0.5671
	IRTV	7.4697	17.4141	27.3986	37.4060	30.6324	23.2822	19.3444	16.6427	0.9471	0.8151	0.6936	0.5882
	ETV	**6.9648**	17.8558	27.7362	37.8116	**31.2232**	23.0625	19.2373	16.5475	0.9422	0.8102	0.6886	0.5861
	Proposed	7.8842	**16.9271**	**26.9387**	**36.9306**	30.1670	**23.5287**	**19.5095**	**16.7653**	**0.9534**	**0.8230**	0.6976	**0.5938**
CT3	DTV	8.1841	18.1538	28.1277	37.9715	29.8411	22.9201	19.1163	16.5092	0.8702	0.6649	0.5480	0.4788
	CDTV	8.5483	**16.8861**	28.5513	38.5108	29.4595	**23.5497**	18.9883	16.3875	0.8618	0.6567	0.5468	0.4767
	NCTV	9.3043	19.2348	29.2041	39.1955	28.7274	22.4204	18.7901	16.2338	0.8411	0.6457	**0.5597**	0.4722
	SBTV	9.9693	19.8947	29.9134	39.8088	28.1256	22.1220	18.5845	16.1000	0.8258	0.6395	0.5343	0.4692
	IRTV	7.4694	17.4209	27.3837	37.3879	30.6330	23.2785	19.3486	16.6475	0.8869	0.6785	0.5568	0.4824
	ETV	7.9006	17.8431	27.7387	37.8122	30.1490	23.0714	19.2376	16.5473	0.8774	0.6674	0.5528	0.4798
	Proposed	**6.9745**	18.5630	**26.8968**	**36.8509**	**31.2272**	22.7271	**19.5047**	**16.7670**	**0.8988**	**0.6858**	0.5588	**0.4872**
CT4	DTV	8.1690	18.0980	28.1172	38.0365	29.8542	22.9476	19.1196	16.4963	0.9361	0.7952	0.6608	0.5480
	CDTV	8.5822	18.5219	28.4912	38.3817	29.4288	22.7422	19.0063	16.4156	0.9306	0.7897	0.6570	**0.5560**
	NCTV	9.2276	19.2467	29.1440	39.1438	28.7928	22.4103	18.8110	16.2462	0.9207	0.7776	0.6450	0.5412
	SBTV	9.9744	19.8810	29.7766	39.9005	28.1205	22.1312	18.6235	16.0812	0.9121	0.7702	0.6393	0.5305
	IRTV	7.4606	17.4154	**26.9256**	37.2329	30.6432	23.2788	**19.4924**	16.6792	0.9450	0.8025	0.6680	0.5557
	ETV	7.8834	17.8268	27.8366	37.7518	30.1645	23.0779	19.2071	16.5582	0.9396	0.7987	0.6653	0.5494
	Proposed	**6.9708**	**16.9406**	27.4470	**36.8389**	**31.2347**	**23.5212**	19.3333	**16.7741**	**0.9519**	**0.8105**	**0.6735**	0.5498

satisfactory results to reduce the Gaussian noise from CT images but failed to preserve the edges over the strong noisy edges. The DTV method gives better SSIM value only over the CT2 image with noise level 30. The ETV method provides smooth edges over the homogeneous regions. However, as noise increases, the edges get blurred. The ETV method gives better RMSE and PSNR values only over the CT2 image with noise level 10. The NCTV method is also helpful to reduce the Gaussian noise from CT images, but, visually texture is not as good as required for clinical purpose. However, the NCTV method gives better SSIM value only over the CT3 image with noise level 30 and Entropy Difference (ED) value only over the CT3 image with noise level 10. The results of CDTV, IRTV and SBTV methods indicate that the noise from CT images is effectively reduced. From experimental analysis, it was analyzed that the results of CDTV method are not sufficiently reduce the higher noise. However, the CDTV method gives some better results such as RMSE and PSNR values over the CT3 image with noise level 20, SSIM value over the CT4 image with noise level 40, and ED value over the CT2 image with noise level 20, as shown in Tables 1 and 1. The SBTV and IRTV methods failed to provide the smoothness over the homogeneous regions, which can be analyzed from Figs. 6 and 7. As noise increases, SBTV method also fails to preserve the textures. However, the SBTV method gives better ED value over the CT1 image with noise level 20. While, the IRTV method also gives some better results such as ED and GMSD values over the CT4 image with noise level 20, SSIM and DIV values over the CT1 image with noise level 20, RMSE and PSNR values over the CT4 image with noise level 30. The results of the proposed scheme provide better outcome for effective noise reduction on the CT images. The edges and texture are well-preserved without over-smoothing or generating the unwanted denoising flaws. In most of the cases, the proposed method gives better RMSE, PSNR, SSIM, ED, DIV and GMSD values over given CT image dataset, as shown in Tables 1 and 1. For more sophisticated CT images, physicians generally prefer original noisy images more willingly in comparison to over-smoothed images. The proposed algorithm provides less smoother

Table 2
ED, DIV and GMSD of CT denoised images.

		ED				DIV				GMSD			
Image	σ	10	20	30	40	10	20	30	40	10	20	30	40
CT1	DTV	0.6618	0.5657	0.5396	0.5233	1.4230	3.2890	5.0488	6.9309	0.0794	0.2065	0.2826	0.3269
	CDTV	0.6547	0.5681	0.5367	0.5228	1.4849	3.1835	4.8124	6.4410	0.0833	0.2093	0.2834	0.3289
	NCTV	0.6436	0.5619	0.5368	0.5222	1.5318	3.5606	5.0399	6.7116	0.0955	0.2167	0.2873	0.3313
	SBTV	0.6276	**0.5572**	0.5359	0.5227	1.6782	3.4186	5.4367	6.9713	0.1053	0.2221	0.2921	0.3328
	IRTV	0.6771	0.5707	0.5375	0.5236	1.4013	**2.8137**	4.5955	6.6144	0.0688	0.1974	0.2770	**0.3240**
	ETV	0.6691	0.5674	0.5368	0.5237	1.4874	3.1870	4.9947	6.5835	0.0738	0.2019	0.2805	0.3285
	Proposed	**0.6213**	0.5739	**0.5313**	**0.5219**	**1.2270**	2.9833	**4.7102**	**6.4088**	**0.0617**	**0.1945**	**0.2740**	0.3248
CT2	DTV	0.2160	0.1866	0.1917	0.2122	2.0167	4.3235	7.0097	9.7046	0.0571	0.1569	0.2199	0.2599
	CDTV	0.2129	**0.1846**	0.1904	0.2165	2.0869	4.6213	7.0424	9.2240	0.0624	0.1577	0.2233	0.2605
	NCTV	0.2105	0.1862	0.1930	0.2170	2.2377	4.8857	7.1624	10.1340	0.0692	0.1623	0.2236	0.2628
	SBTV	0.2045	0.1858	0.1962	0.2190	2.4397	5.0360	7.5028	9.8770	0.0771	0.1709	0.2273	0.2650
	IRTV	0.2226	0.1872	0.1880	0.2115	1.8326	4.2262	6.7563	9.4507	0.0502	0.1487	0.2172	0.2578
	ETV	0.2184	0.1869	0.1899	0.2139	1.9644	4.3427	7.0746	9.6899	0.0550	0.1515	0.2176	0.2588
	Proposed	**0.2037**	0.1885	**0.1878**	**0.2099**	**1.7305**	**4.3030**	**6.4731**	**9.0947**	**0.0459**	**0.1466**	**0.2137**	**0.2547**
CT3	DTV	0.6924	0.5971	0.5737	0.5686	3.7617	8.7158	13.5662	18.4269	0.0796	0.2060	0.2781	0.3194
	CDTV	0.6865	0.5950	0.5755	0.5698	4.0448	8.9458	13.6403	17.8657	0.0860	0.2100	0.2809	0.3201
	NCTV	**0.6739**	0.5928	0.5726	0.5675	4.3108	9.2104	14.0623	18.8141	0.0973	0.2153	0.2838	0.3236
	SBTV	0.6810	0.5879	0.5792	0.5683	4.7438	9.0988	14.0902	19.3326	0.1064	0.2223	0.2878	0.3243
	IRTV	0.7080	0.5991	0.5735	0.5667	3.6907	8.2033	12.1909	17.6931	0.0710	0.1961	0.2735	0.3166
	ETV	0.6987	0.5997	0.5738	0.5664	3.8453	8.7534	13.2321	18.1521	0.0768	0.2026	0.2753	0.3185
	Proposed	0.6940	**0.5846**	**0.5716**	**0.563**6	**3.1779**	**7.9014**	**13.1541**	**16.8782**	**0.0634**	**0.1921**	**0.2720**	**0.3152**
CT4	DTV	0.2180	0.1853	0.1852	0.2040	1.8633	4.3152	6.5716	8.5008	0.0580	0.1540	0.2193	0.2583
	CDTV	0.2139	0.1855	0.1867	0.2037	2.0693	4.2925	6.8359	8.9685	0.0630	0.1583	0.2216	0.2588
	NCTV	0.2087	0.1856	0.1881	0.2073	2.1010	4.3883	6.8031	9.2242	0.0698	0.1640	0.2234	0.2600
	SBTV	0.2176	0.1852	0.1886	0.2087	2.4249	4.7364	7.0283	9.2779	0.0774	0.1669	0.2257	0.2635
	IRTV	0.2229	**0.1840**	0.1859	0.2025	1.8446	4.1105	6.3610	8.4685	0.0510	0.1497	**0.2147**	0.2551
	ETV	0.2185	0.1863	0.1860	0.2027	1.8374	4.2139	6.6262	8.8953	0.0543	0.1507	0.2167	0.2575
	Proposed	**0.2049**	0.1849	**0.1842**	**0.2017**	**1.6181**	**3.8725**	**6.3447**	**8.4888**	**0.0441**	**0.1433**	0.2148	**0.2548**

results with preserved edges and reduced noise which can be helpful for clinical purpose.

A zoom cropped object of low contrast noisy CT2 image as shown in figure in 10(a) is also used to verify the performance of the proposed algorithm. Fig. 10(b), (c), (d), (e), (f), (g) and (h) are the results of DTV, CDTV, NCTV, SBTV, IRTV, ETV and the proposed method, respectively. Visually, it can be analyzed that the proposed method gives better outcomes in terms of noise reduction and better edge preservation. For more critical analysis of noise reduction from noisy CT image, the profile of CT3 image is also obtained to compute the intensity values along a line. The analysis of the profiles of denoised CT image as shown in Fig. 11 indicates

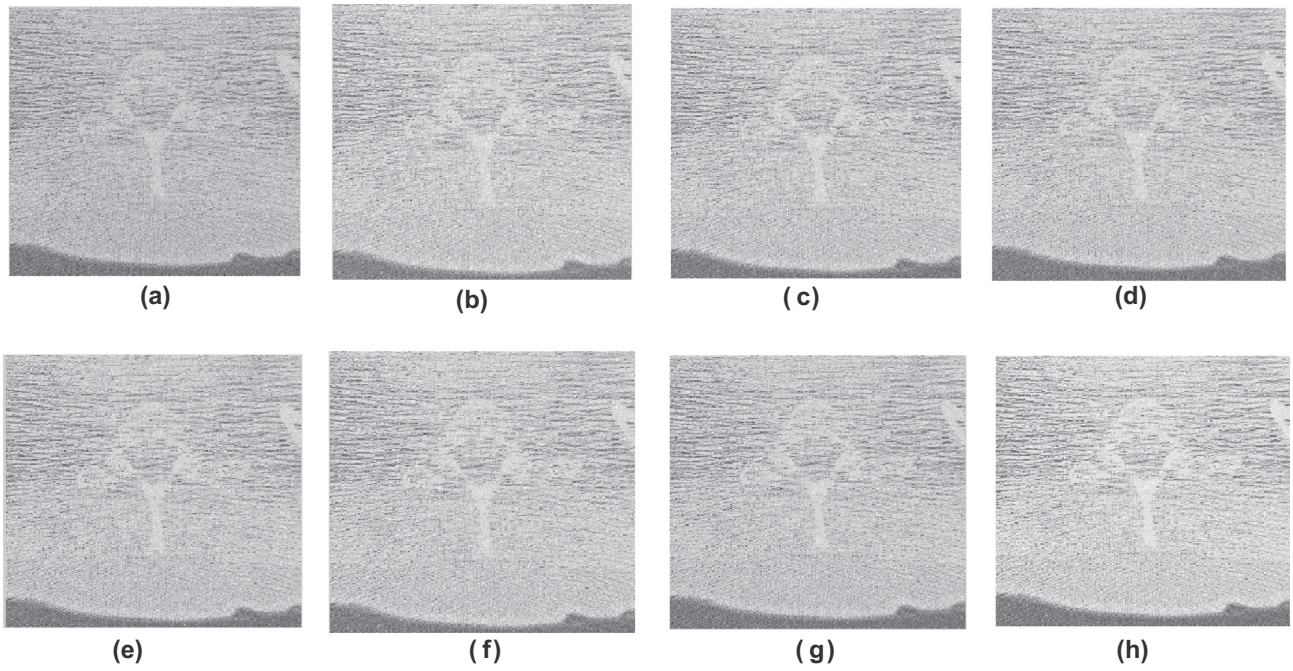

Fig. 10. Analysis on zoomed image of noisy CT2 image: (a) zoomed image of noisy CT2; (b) result of DTV; (c) result of CDTV; (d) result of NCTV; (e) result of SBTV; (f) result of IRTV; (g) result of ETV; and (h) result of proposed algorithm.

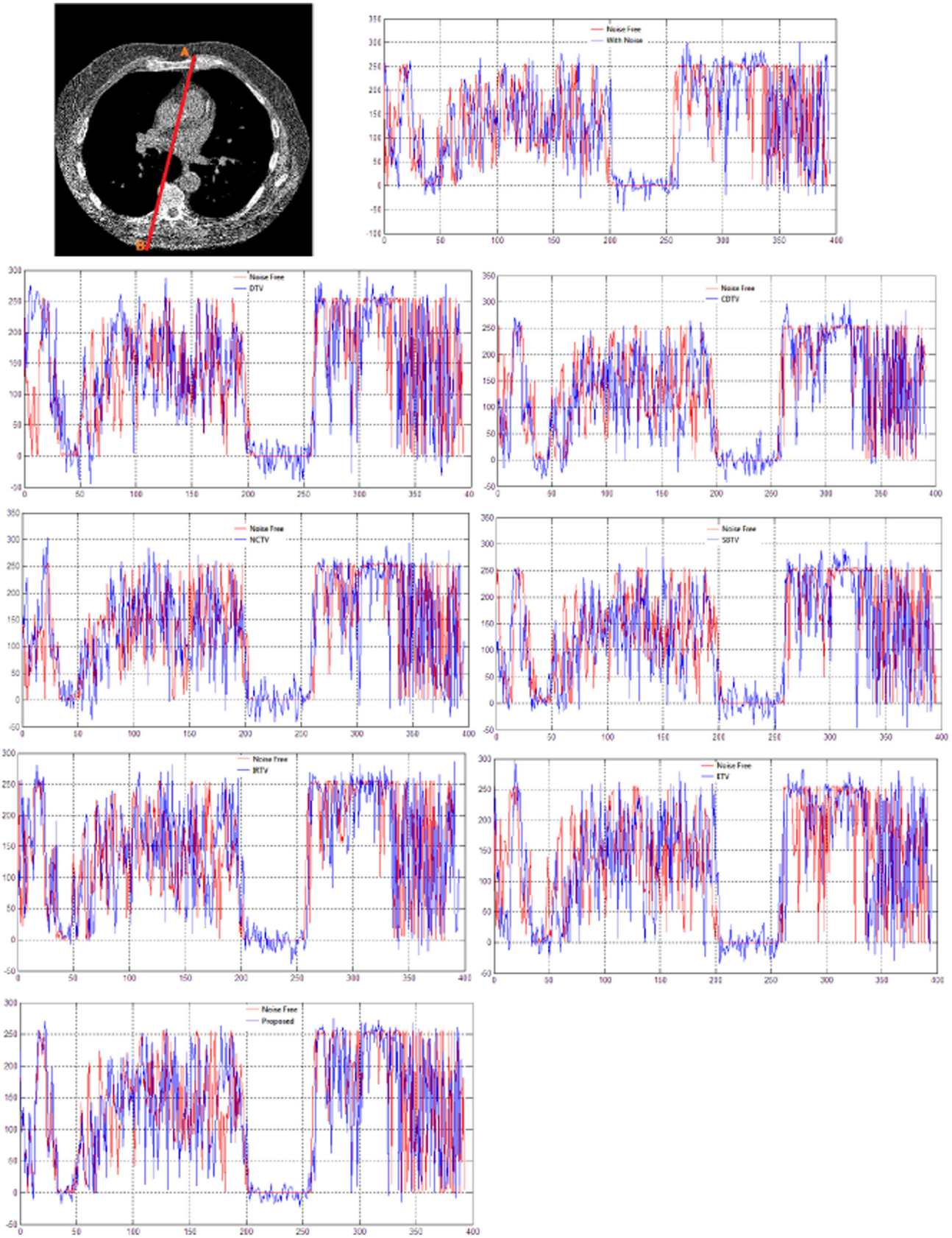

Fig. 11. Intensity profile of a line on CT3 image. In each plot, the Noise Free intensity profile is plotted in red and filtered profile is plotted in blue.

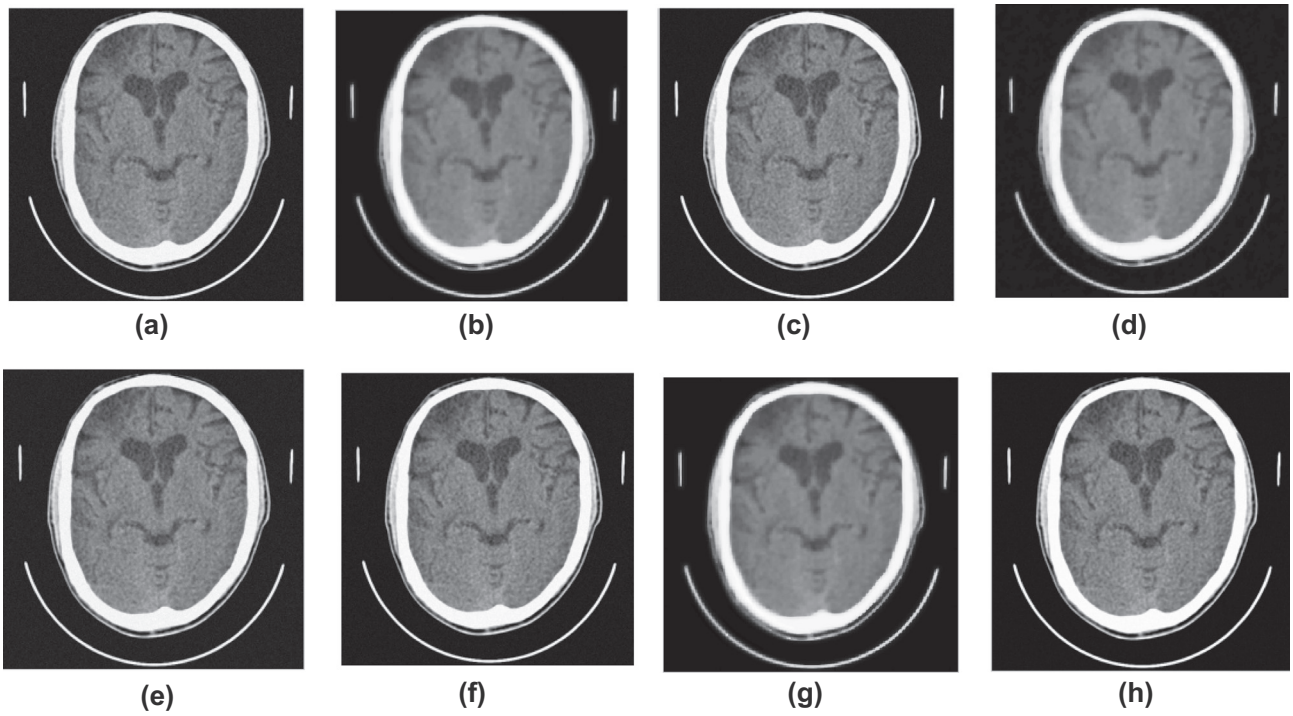

Fig. 12. Analysis on real noisy CT image: (a) real noisy CT image; (b) result of DTV; (c) result of CDTV; (d) result of NCTV; (e) result of SBTV; (f) result of IRTV; (g) result of ETV; and (h) result of proposed algorithm.

Table 3
Execution time for different denoising methods (in seconds).

Method	DTV	CDTV	NCTV	SBTV	IRTV	ETV	Proposed
Time	15.4976	3.3612	3.3125	.5667	2.9831	6.7121	3.0195

that the proposed scheme is better in comparison to existing denoising schemes.

The computation time is also an important factor to measure the performance of the proposed methods. The average computation time in second(s) of proposed method and compared methods are shown in Table 3. From Table 3, it can be observed that the proposed method takes relatively less computation time in comparison to DTV, CDTV, NCTV and ETV methods but slightly more time compared to SBTV and IRTV methods. As the number of iterations is increased, the time cost is proportionally increased. However, the proposed method still takes lesser computation time in comparison to DTV, CDTV and ETV methods. Hence, there is trade-off between the performance and computation time in the proposed scheme. The major difficulty of deriving the results is to find the optimum values of the inner parameters (α, β, μ). However, it can be resolved by setting default values of inner parameters to perform the proposed algorithm iteratively. The results can slightly vary by changing the inner parameter values of the proposed scheme.

5. Conclusions

In this article, a new exponentially directional weighted function (EDWF) for anisotropic and isotropic TV is developed to denoise the computed tomography medical images. The performance of the proposed method is evaluated with various factors such as visual inspection of real CT image (added noisy and real noisy). The performance metrics such as RMSE, PSNR, SSIM, ED, DIV and GMSD are also computed and compared. From comparison and result analysis, it can be clearly said that the proposed method recovers visually accepted image by preserving most of the structures with less computation time. It also preserves the small image details and generates no visual artifacts. The performance of the proposed algorithm has a great potential to serve for denoising the computed tomography images.

References

Al-Ameen, Zohair, Sulong, Ghazali, 2014. Attenuating noise from computed tomography medical images using a coefficients-driven total variation denoising algorithm. Int. J. Imaging Syst. Technol. 24 (4), 350–358.
Ali, S.A., Vathsal, S., Kishore, K.L., 2010. Efficient denoising technique for CT Images using Window based multi-wavelet transformation and thresholding. Eur. J. Sci. Res. 48, 315–325.
Andrews, H.C., Hunt, B.R., 1997. Digital image restoration. IEEE Signal Process. Mag. 24–41.
Andria, G., Attivissimo, F., Lanzolla, A.M.L., 2013. A statistical approach for MR and CT images comparison. Measurement 46, 57–65.
Attivissimo, F., Cavone, G., Lanzolla, A.M.L., Spadavecchia, M., 2010. A technique to improve the image quality in computer tomography. IEEE Trans. Instrum. Meas. 59, 1251–1257.
Bayram, Ilker, Kamasak, Mustafa E., 2012. Directional total variation. IEEE Signal Process. Lett. 19 (12), 781–784.
Beck, A., Teboulle, M., 2009. Fast gradient-based algorithms for constrained total variation image denoising and deblurring problems. IEEE Trans. Image Process. 18 (11), 2419–2434.
Bhadauria, H.S., Dewal, M.L., 2012. Efficient denoising technique for CT images to enhance brain hemorrhage segmentation. J. Digit Imaging 25, 782–791.
Borsdorf, A., Raupach, R., Flohr, T., Hornegger, J., 2008. Wavelet based noise reduction in CT-images using correlation analysis. IEEE Trans. Med. Imaging 27 (12), 1685–1703.
Cai, J.F., Osher, S., Shen, Z., 2009a. Convergence of the linearized Bregman iteration for L1-norm minimization. Math. Comput. 78, 2127–2136.
Cai, J.F., Osher, S., Shen, Z., 2009b. Linearized Bregman iterations for compressed sensing. Math. Comput. 78, 1515–1536.
Cai, J.F., Oshert, S., Shen, Z.W., 2009c. Split Bregman methods and frame based image restoration. SIAM Multiscale Model. Simul. 8 (2), 337–369.
Candes, E., Wakin, M., Boyd, S., 2008. Enhancing sparsity by reweighted 1 minimization. J. Fourier Anal. Appl. 14 (5), 877–905.
Catt, F., Lions, P.-L., Morel, J.-M., Coll, T., 1992. Image selective smoothing and edge detection by nonlinear diffusion. SIAM J. Numer. Anal. 29 (1), 182–193.
Rudin, L., Osher, S., Total variation based image restoration with free local constraints. In: Proc. IEEE Int. Conf. Image Process., 1994, 31–35.

Chambolle, A., 2004. An algorithm for total variation minimization and applications. J. Math. Imag. Vis. 20, 89–97.
Chambolle, A., Pock, T., 2011. A first-order primaldual algorithm for convex problems with applications to imaging. J. Math. Imag. Vis. 40 (1), 120–145.
Chen, Huasong, Wang, Chunyong, Song, Yang, Li, Zhenhua, 2015. Split Bregmanized anisotropic total variation model for image deblurring. J. Visual Commun. Image Represent. 31, 282–293.
Darbon, J., Sigelle, M., 2006. Image restoration with discrete constrained total variation Part I: fast and exact optimization. J. Math. Imag. Vis. 26, 261–276.
Denis, L., Tupin, F., Darbon, J., Sigelle, M., 2009. SAR image regularization with fast approximate discrete minimization. IEEE Trans. Image Process. 18 (7), 1588–1600.
Dobson, D.C., Santosa, F., 1996. Recovery of blocky images from noisy and blurred data. SIAM J. Appl. Math. 56, 1181–1198.
Esedoglu, Selim, Osher, Stanley J., 2004. Decomposition of images by the anisotropic RudinOSherFatemi model. Commun. Pure Appl. Math. LVII, 1609–1626.
Fathi, A., Naghsh Nilchi, A.R., 2012. Efficient image denoising method based on a new adaptive wavelet packet thresholding function. IEEE Trans. Image Process. 21 (9), 3981–3990.
Goldstein, Tom, Osher, Stanley, 2009. The split Bregman method for L1-regularized problems. SIAM J. Imag. Sci. 2 (2), 323–343.
Gravel, P., Beaudoin, G., De Guise, J.A., 2004. A method for modeling noise in medical images. IEEE Trans. Med. Imaging 23, 1221–1232.
Hu, Y., Jacob, M., 2012. Higher degree total variation (hdtv) regularization for image recovery. IEEE Trans. Image Process. 21 (5), 2559–2571.
Yan, J., Lu, W.-S., New algorithms for sparse representation of discrete signals based on p-2 optimization. In Proc. IEEE PacRim Conf. 2011, 73–78.
Yan, J., Lu, W.-S., Power-iterative strategy for p-2 optimization for compressive sensing: towards global solution. In Proc. IEEE Asilomar Conf. 2011, 1153–1157.
Yan, J., Lu, W.-S., Smoothed p-2 Solvers for Signal Denoising. In Proc. IEEE ICASSP Conf. 2012, 3801–3804.
Hu, J., Wang, Z., Shen, B., Gao, H., 2013a. Quantised recursive filtering for a class of nonlinear systems with multiplicative noises and missing measurements. Int. J. Control 86 (4), 650–663.
Hu, J., Wang, Z., Shen, B., Gao, H., 2013b. Gain-constrained recursive filtering with stochastic nonlinearities and probabilistic sensor delays. IEEE Trans. Signal Process. 61 (5), 1230–1238.
Hu, J., Wang, Z., Liu, S., Gao, H., 2016. A variance-constrained approach to recursive state estimation for time-varying complex networks with missing measurements. Automatica 64, 155–162.
Jiang, Wenfei, Cui, Hengbin, Zhang, Fan, Rong, Yaocheng, Chen, Zhibo, 2015. Oriented total variation l1/2 regularization. J. Visual Commun. Image Represent. 29, 125–137.
Kumar, M., Diwakar, M., 2016. CT image denoising using locally adaptive shrinkage rule in tetrolet domain. J. King Saud Univ.-Comput. Inf. Sci. https://doi.org/10.1016/j.jksuci.2016.03.003.
Landi, German, Loli Piccolomini, E., 2012. An efficient method for nonnegatively constrained Total Variation-based denoising of medical images corrupted by Poisson noise. Comput. Med. Imaging Graphics 36 (1), 38–46.
Li, WeiHong, Li, Quanli, Gong, Weiguo, Tang, Sh.u., 2012. Total variation blind deconvolution employing split Bregman iteration. J. Vis. Commun. Image R. 23, 409–417.
Lou, Y., Zeng, T., Osher, S., Xin, J., 2015. A weighted difference of anisotropic and isotropic total variation model for image processing. SIAM J. Imaging Sci. 8 (3), 1798–1823.
Muller, P., Hiller, J., Cantatore, A., De Chiffre, L., 2012. A study on evaluation strategies in dimensional X-ray computed tomography by estimation of measurement uncertainties. Int. J. Metrol. Qual. Eng. 3, 107–115.
Naimi, H., Adamou-Mitiche, A.B.H., Mitiche, L., 2015. Medical image denoising using dual tree complex thresholding wavelet transform and Wiener filter. J. King Saud Univ.-Comput. Inf. Sci. 27 (1), 40–45.
Nikolova, M., 2000. Local strong homogeneity of a regularized estimator. SIAM J. Appl. Math. 61, 633–658.
Osher, Stanley, Burgery, Martin, Goldfarb, Donald, Jinjun, Xu., Yin, Wotao, 2005. An iterative regularization method for total variation based image restoration. SIAM Multiscale Model. Simul. 4 (2), 460–489.
Perona, P., Malik, J., 1990. Scale space and edge detection using anisotropic diffusion. IEEE Trans. Pattern Anal. Mach. Intell. 12 (7), 629–639.
Rudin, L., Osher, S., Fatemi, E., 1992. Nonlinear total variation based noise removal algorithms. Physica D 60, 259–268.
Sanches, J.M., Nascimento, J.C., Marques, J.S., 2008. Medical image noise reduction using the SylvesterLyapunov equation. IEEE Trans. Image Process. 17, 1522–1539.
Sun, Y., Zhang, L., Zhang, J., Shi, L., 2013. Neural network blind equalization algorithm applied in medical CT image restoration. Math. Probl. Eng.
Sun, Chen, Tang, Chen, Zhu, Xinjun, Ren, Hongwei, 2015. Exponential total variation model for noise removal, its numerical algorithms and applications. AEU-Int. J. Electron. Commun. 69 (3), 644–654.
Tikhonov, A.N., Arsenn, V.Y., 1977. Solutions of Ill-Posed Problems. Scripta Series in Mathematics. V.H. Winston and Sons; John Wiley and Sons, Washington, D.C., New York.
Trinh, D.H., Luong, M., Rocchisani, J., Pham, C.D., Pham, H.D., Dibos, F., 2012. An optimal weight method for CT image denoising. J. Electron. Sci. Technol. 10, 124–129.
Vogel, C., 1995. A multigrid method for total variation-based image denoising. Computation and Control IV, Progress in Systems and Control Theory, vol. 20. Birkhauser.
Vogel, C., Oman, M., 1996. Iterative methods for total variation denoising. SIAM J. Sci. Comput. 17, 227–238.
Wang, Zhou, Bovik, Alan Conrad, Sheikh, Hamid Rahim, Simoncelli, Eero P., 2004. Image quality assessment: from error visibility to structural similarity. IEEE Trans. Image Process. 13 (4), 600–612.
Weickert, J., 1998. Anisotropic Diffusion in Image Processing. Teubner Stuttgart.
Wu, H., Zhang, W., Gao, D., Yin, X., Chen, Y., Wang, W., 2011. Fast CT image processing using parallelized non-local means. J. Med. Biol. Eng. 31, 437–441.
Wu, Y., Tracey, B., Natarajan, P., Noonan, J.P., 2013a. JamesStein type center pixel weights for non-local means image denoising. IEEE Signal Process. Lett. 20, 411–414.
Wu, Y., Tracey, B., Natarajan, P., Noonan, J.P., 2013b. Probabilistic non-local means. IEEE Signal Proces. Lett. 20, 763–766.
Xue, Wufeng, Zhang, Lei, Mou, Xuanqin, Bovik, Alan C., 2014. Gradient magnitude similarity deviation: a highly efficient perceptual image quality index. IEEE Trans. Image Process. 23 (2), 684–695.
Yan, Jie, Wu-Sheng, Lu., 2015. Image denoising by generalized total variation regularization and least squares fidelity. Multidimensional Syst. Signal Process. 26 (1), 243–266.
Yin, W., Osher, S., Goldfarb, D., Darbon, J., 2008. Bregman iterative algorithms for L1-minimization with applications to compressed sensing. SIAM J. Imag. Sci. 1, 143–168.
Zhu, F., Carpenter, T., Gonzalez, D.R., Atkinson, M., Wardlaw, J., 2012. Computed tomography perfusion imaging denoising using Gaussian process regression. Phys. Med. Biol. 57, N183.
Zibulevsky, M., Elad, M., 2012. L1–L2 optimization in signal and image processing. IEEE Signal Process. Mag. 27 (3), 76–88.